Membrane heterogeneities in the formation of B cell receptor–Lyn kinase microclusters and the immune synapse

Hae Won Sohn, Pavel Tolar, and Susan K. Pierce

Laboratory of Immunogenetics, National Institute of Allergy and Infectious Diseases, National Institutes of Health, Rockville, MD 20852

Antigen binding to the B cell receptors (BCRs) induces BCR clustering, phosphorylation of BCRs by the Src family kinase Lyn, initiation of signaling, and formation of an immune synapse. We investigated B cells as they first encountered antigen on a membrane using live cell high resolution total internal reflection fluorescence microscopy in conjunction with fluorescence resonance energy transfer. Newly formed BCR microclusters perturb the local membrane microenvironment, leading to association with a lipid raft probe. This early event is BCR intrinsic and independent of BCR signaling. Association of BCR microclusters with membrane-tethered Lyn depends on Lyn activity and persists as microclusters accumulate and form an immune synapse. Membrane perturbation and BCR–Lyn association correlate both temporally and spatially with the transition of microclustered BCRs from a "closed" to an "open" active signaling conformation. Visualization and analysis of the earliest events in BCR signaling highlight the importance of the membrane microenvironment for formation of BCR–Lyn complexes and the B cell immune synapse.

Introduction

Binding of antigens to the B cell receptors (BCRs) leads to clustering of the BCRs and triggering of a signaling cascade resulting in the activation of a variety of genes associated with B cell activation (Cambier et al., 1994; Reth and Wienands, 1997; Dal Porto et al., 2004; Hou et al., 2006). We now understand the biochemical nature of the BCR's signaling pathway beginning with phosphorylation of the BCR by the first kinase in the signaling cascade, the membrane-associated Lyn, in considerable detail. However, what remains only poorly understood are the very earliest events that follow antigen-induced clustering of the BCRs that lead to association of the BCR with Lyn and triggering of the signaling cascade. Of particular interest are the potential roles of plasma membrane lipid heterogeneities and the local lipid microenvironment of the BCR in the initiation of signaling. Indeed, Lyn is acylated by both myristoylation and palmitoylation that both dictate Lyn's membrane localization and are essential for Lyn's function (Kovarova et al., 2001). The results of previous biochemical studies using detergent solubility to identify membrane microenvironments suggested that lipid heterogeneities may play an important role in the initiation of B cell signaling by regulating access of the BCR to Lyn (Cheng et al., 1999; Aman and Ravichandran, 2000; Guo et al., 2000). These studies provided evidence that detergent-insoluble, sphingolipid-rich, and cholesterol-rich membrane microdomains termed lipid rafts concentrate the membrane-tethered dually acylated Lyn kinase and, in so doing, potentially provide a platform for BCR signaling. Subsequently, using fluorescence resonance energy transfer (FRET) confocal microscopy in live B cells, we showed that within seconds of the B cell's encounter with soluble antigens, the BCR transiently associated with a lipid raft probe, a myristoylated and palmitoylated fluorescent protein present in the detergent-insoluble lipid raft fraction of the plasma membrane (Sohn et al., 2006). This interaction was selective and was not observed with fluorescent proteins that were tethered to the detergent-soluble regions of the membrane by geranylgeranylation or myristoylation and preceded by several seconds the induction of a Ca^{2+} flux. These results are consistent with recent revised models of the original raft hypothesis (Simons and Ikonen, 1997; Edidin, 2003) that take into account the dominant role for plasma membrane proteins in capturing and stabilizing intrinsically unstable lipid domains (Hancock, 2006).

Correspondence to Susan K. Pierce: spierce@nih.gov

Abbreviations used in this paper: APC, antigen-presenting cell; BCR, B cell receptor; FI, fluorescence intensity; FRET, fluorescence resonance energy transfer; ICAM-1, intercellular adhesion molecule-1; ITAM, immunoreceptor tyrosine-based activation motif; LynFL, full-length Lyn; PC, phosphorylcholine; TIRFM, total internal reflection fluorescence microscopy.

The online version of this article contains supplemental material.

The Rockefeller University Press $30.00
J. Cell Biol. Vol. 182 No. 2 367–379
www.jcb.org/cgi/doi/10.1083/jcb.200802007

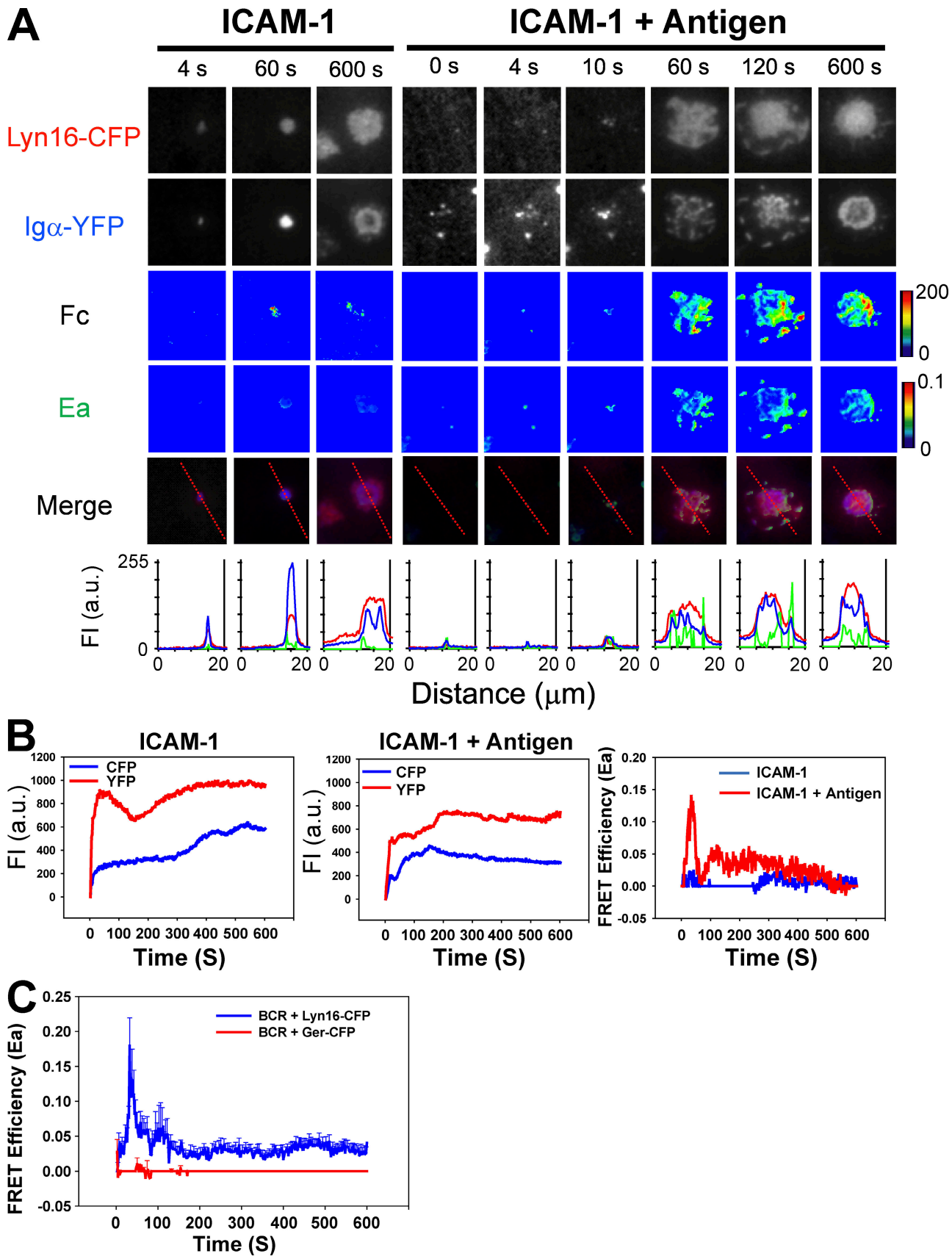

Figure 1. **Time-lapse FRET imaging using TIRFM reveals the spatial and temporal dynamics of the change in the lipid environment of the BCR during antigen contact.** (A) Time-lapse TIRFM images of CH27 B cells expressing Igα-YFP and Lyn16-CFP contacting a planar lipid bilayer containing only ICAM-1 or ICAM-1 and the antigen PC_{10}-BSA. Three-channel TIRFM images were acquired using an electron-multiplier CCD camera. The CFP and YFP images are shown. FRET was calculated by sensitized acceptor emission as described in Materials and methods. Corrected net FRET (Fc = F − β × D − γ × A) and

The finding that the antigen-clustered BCR associated with the lipid raft probe predicted that the association with lipid rafts would lead to interaction of the BCR with Lyn kinase itself. However, this prediction was not tested directly. In addition, these results were acquired by investigating the response of B cells to soluble antigens, and several recent studies provided evidence that the relevant mode of antigen recognition by B cells in vivo may be on the surfaces of antigen-presenting cells (APCs). Indeed, results from a study using intravital two-photon imaging suggest that B cells contact antigen not in solution but rather on the surfaces of APCs in lymphoid organs (Qi et al., 2006). Studies in vitro showed that B cells encountering antigen on the surface of an APC or on a planar lipid bilayer, approximating an APC surface, form an immune synapse (Batista et al., 2001; Carrasco and Batista, 2006; Fleire et al., 2006), a structure associated with B cell activation. In addition, results of a recent study indicate that the requirements for B cell responses to membrane-bound antigens are significantly different from those for responses to soluble antigens (Depoil et al., 2008). Indeed, unlike BCR signaling in response to soluble antigens that is initiated independently of the B cell coreceptor, CD19, response to membrane antigen was defective in the absence of CD19.

To capture the earliest events in the interaction of BCR with the lipid rafts and the membrane-tethered Lyn kinase after contact with antigen in a planar membrane, we took advantage of FRET in conjunction with total internal reflection fluorescence microscopy (TIRFM). TIRFM provided high resolution images that allowed us to observe the formation of individual BCR microclusters and their interaction with a raft lipid probe and with Lyn and relate these to BCR activation and formation of the immune synapse. In this study, we provide evidence that the individual BCR microclusters that first formed after antigen contact perturbed the local membrane microenvironment, leading to association of the clustered BCRs with a raft lipid probe. BCR microclusters interacted with Lyn, an interaction that persisted as the BCR microclusters accumulated and formed an immune synapse. The association with the lipid raft probe and Lyn with BCR clusters correlated in both time and space with the transition of BCR microcluster cytoplasmic domains to an "open" active conformation. These results provide a new view of the dynamic process of antigen-induced BCR microclustering and the effect of microclustering on the local lipid microenvironment and recruitment of Lyn.

Results

Molecular interactions of antigen-induced BCR microclusters with a lipid raft probe

To analyze the BCR's interaction with lipid rafts, B cell lines were generated that were specific for the antigen phosphorylcholine (PC) and stably expressed a chimeric BCR Igα chain that contained the FRET acceptor YFP in its cytoplasmic domain (Igα-YFP) and a FRET donor CFP that contained the first 16 amino acids of the Src family kinase Lyn (Lyn16-CFP), resulting in its myristoylation and palmitoylation and association with the detergent-insoluble fractions of the plasma membrane (Sohn et al., 2006). Previous studies showed that cell lines expressing Igα-YFP and Lyn16-CFP were functional and responded to antigens and established the validity of using FRET measurements to detect molecular interactions between antigen-clustered BCRs and lipid raft probes (Sohn et al., 2006). B cells were placed on a planar lipid bilayer that contained biotinylated forms of either the antigen, PC_{10}-BSA, and the adhesion molecule, intercellular adhesion molecule-1 (ICAM-1), or ICAM-1 alone and were tethered to the lipid bilayer by streptavidin and biotinylated 1,2-dioleoyl-*sn*-glycero-3-phosphoethanolamine. Three-channel TIRF microscope images were acquired (CFP, FRET, and YFP) at 2- or 4-s intervals for 15 min. Influences of the relative concentration of YFP and CFP on the FRET measurements were addressed by calibrating the bleed-through of the donor fluorescence in the acceptor detection channel and the amount of directly excited acceptor fluorescence as previously described (van Rheenen et al., 2004; Zal and Gascoigne, 2004) by measuring the donor and acceptor emissions of cells that contained only the acceptor or donor fluorescent proteins in the same field as the experimental cells. FRET was calculated by sensitized acceptor emission and expressed as either corrected FRET values (Fc) or as FRET efficiency normalized for the acceptor (Ea) as detailed in the Materials and methods section.

B cells placed on a bilayer that contained ICAM-1 alone failed to spread and contacted the bilayer over a relatively small area of $\sim$20 μm^2 (unpublished data). In contrast, on ICAM-1– and antigen-containing bilayers, the B cells spread, forming contact areas of $\sim$80 μm^2. Time-lapse imaging showed that the first contact points of the B cell membrane with the ICAM-1–only bilayer occurred in discrete membrane protrusions that contained both Igα-YFP and Lyn16-CFP (Fig. 1 A). The area of contact grew with time, and although the relative fluorescence intensities (FIs) of Igα-YFP and Lyn16-CFP were similar over the contact area (Fig. 1 B) and overlapped extensively at each time point (Fig. 1 A), at no point in time was there significant FRET between Igα-YFP and Lyn16-CFP. Thus, molecular interactions of the BCR with raft lipids did not occur in the absence of antigen to engage the BCR.

B cells also first contacted the ICAM-1– and antigen-containing lipid bilayers through multiple, small points (Fig. 1 A). Both Lyn16-CFP and Igα-YFP were visible in these early contact points, and FRET was detected between Igα-YFP and Lyn16-CFP, indicating that the earliest antigen-induced BCR microclusters associated with the lipid raft probe. With time, the B cells spread on the bilayer, concentrating the BCR Igα-YFP

FRET efficiency from representative cells are shown as color-coded scaled images. A merged image of CFP (red), YFP (blue), and Ea (green) is also shown, and the relative FIs across the cells indicated by red lines (scale, 20 μm) are given. (B) FIs of Igα-YFP, Lyn16-CFP, and FRET efficiencies with time for the cells imaged in A. Note that a 10:1 ratio of CFP to YFP FIs is equivalent to a 1:1 molar ratio of CFP to YFP under our experimental setting as described in Materials and methods. (C) Mean + SEM (error bars) of the FRET efficiencies for multiple cells expressing Igα-YFP and either Lyn16-CFP (12 cells) or Ger-CFP (six cells). The data are from one of three independent experiments.

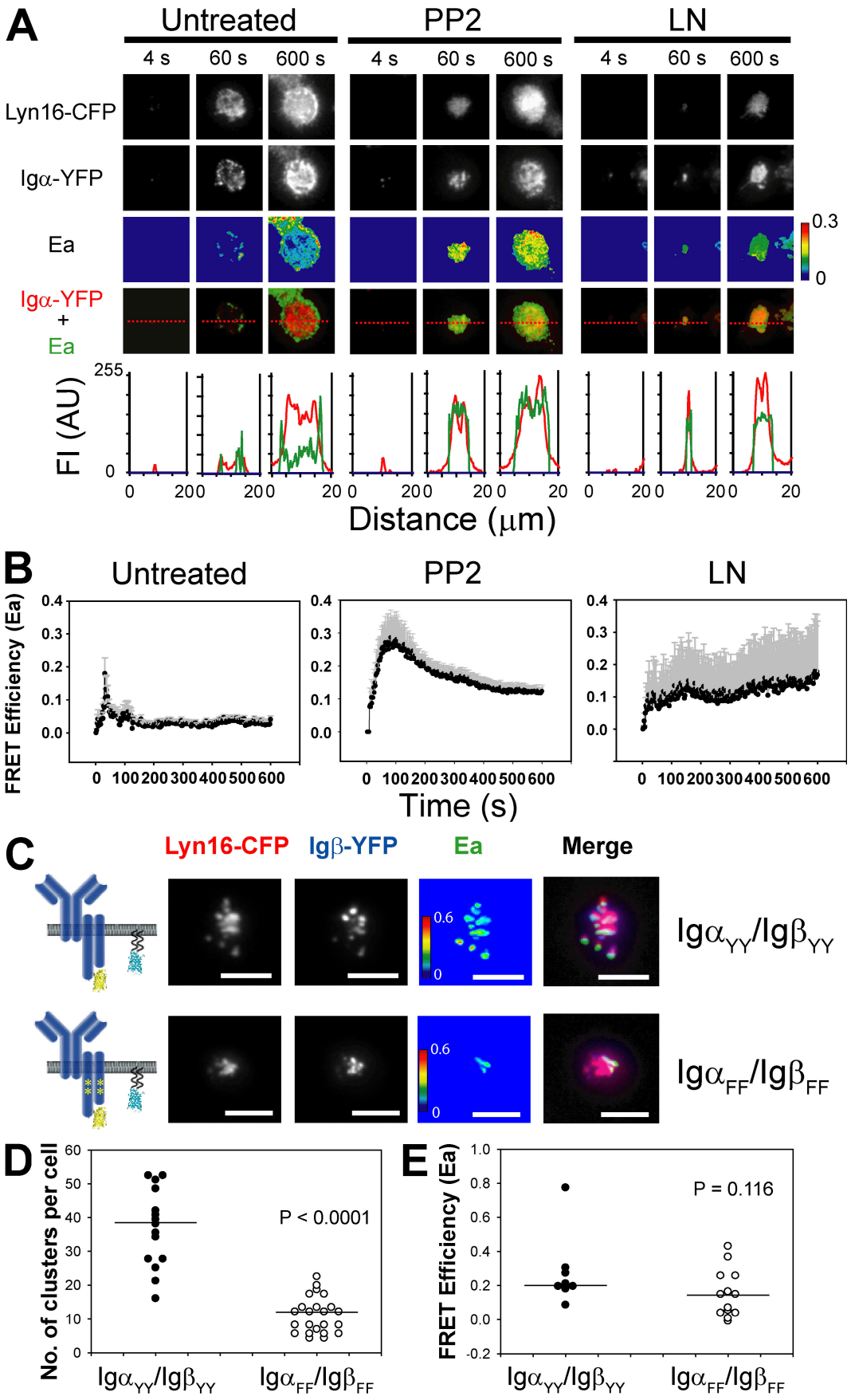

Figure 2. **The interactions of BCR clusters and the raft lipid probe are not dependent on the initiation of BCR signaling or on the actin cytoskeleton.** (A) CFP, YFP, and Ea time-lapse images (acquired as in Fig. 1) of CH27 B cells expressing Igα-YFP and the raft lipid probe, Lyn16-CFP, at 4, 60, and 600 s after

and Lyn16-CFP in the center of the contact area and subsequently contracting, forming a mature synapse. As BCR microclusters were concentrated in the synapse, new B cell clusters continued to form in the periphery of the B cells' contact area and then moved to the center synapse. Notably, the highest FRET values detected were not in the center of the synapse where Igα-YFP and Lyn16-CFP were most concentrated, but rather FRET was highest in the periphery of the B cell's contact area with the bilayer, where there was relatively little accumulation of Igα-YFP and Lyn16-CFP but where new BCR-antigen clusters continued to form (Fig. 1 A). Thus, the difference in FRET values in the cell's periphery versus in the synapse could not be attributed to the concentration of Igα-YFP relative to Lyn16-CFP. Similarly, the relative FIs of Igα-YFP and Lyn16-CFP over the contact area were similar with time for cells engaging either ICAM-1 alone or ICAM-1 and antigen, yet FRET was only observed in cells contacting ICAM-1 and antigen (Fig. 1 B). Moreover, the FRET between Igα-YFP and Lyn16-CFP was specific and did not occur between Igα-YFP and Ger-CFP (Fig. 1 C) that contained the C-terminal polybasic12 residues of K-ras and four residues of rap1B, resulting in CFP's geranylgeranylation and, as previously shown, targeting to nonraft detergent-soluble membranes (Pyenta et al., 2001; Sohn et al., 2006). Collectively, these data provide evidence for a selective molecular interaction between the antigen-clustered BCRs and the lipid raft probe.

Association of the antigen-clustered BCRs with raft lipids is independent of signaling and association with the actin cytoskeleton

To determine whether association of the clustered BCRs with the raft lipid probe was dependent on either signaling or the function of the actin cytoskeleton, B cells were treated with either PP2 to inhibit Src family kinases (Hanke et al., 1996) or with latrunculin B to disassemble the actin cytoskeleton (Brown and Song, 2001) before exposure to ICAM-1– and antigen-containing bilayers. Our previous study showed that PP2 blocked FRET between Igα-CFP and Lyn16-YFP in cells encountering antigen in solution (Sohn et al., 2006). Here, we found that although PP2 affected the ability of B cells to both spread on the bilayer and organize the BCR in a synapse, it did not block FRET between Igα-YFP and Lyn16-CFP upon BCR antigen binding (Fig. 2 A). Thus, association of the BCR with raft lipids showed different requirements for Src family kinase activity when the B cell engaged antigen in solution versus on a membrane. The requirement of Src family kinase activity when antigen is bound from solution may reflect a role of these kinases in maintaining some feature of the cell membrane or local membrane topology, requirements that contact between the B cell membrane and the antigen-containing bilayer overcomes. In addition, although PP2 does not block FRET between Igα-YFP and Lyn16-CFP, both the FRET spatial and kinetic patterns were altered by treatment with PP2 (Fig. 2, A and B), presumably reflecting a requirement for Src family kinase activity in these downstream processes. Similar results were obtained in cells treated with latrunculin B. FRET between Igα-YFP and Lyn16-CFP was observed after antigen-induced BCR clustering, but both the kinetics and spatial pattern of FRET were affected as compared with untreated cells. Collectively, these observations indicate that association of the BCRs with raft lipids that occurs within the first several seconds of BCR-antigen engagement is independent of signaling and association with the actin cytoskeleton. However, importantly, failure to either signal or associate with the actin cytoskeleton significantly affected both the spatial distribution and kinetics of the BCR–lipid raft probe interactions by mechanisms that remain to be elucidated.

To independently confirm that BCR signaling was not required for the association of BCR clusters with raft lipids, we analyzed two previously described NIP (4-hydroxy-5-iodo-3-nitrophenyl acetyl)-specific J558L B cell lines expressing Lyn16-CFP and either a wild-type BCR or a signaling-incompetent BCR in which the two tyrosines within the cytoplasmic immunoreceptor tyrosine-based activation motif (ITAM) of Igα and Igβ chains were mutated to phenylalanine (Tolar et al., 2005). The B cells expressing the ITAM mutant BCR failed to spread on the antigen- and ICAM-1–containing bilayer (Fig. 2 C) and formed fewer BCR microclusters as compared with the wild-type receptor (Fig. 2 D). However, the BCR Igβ-YFP clusters that formed showed FRET with Lyn16-CFP that was comparable with that of the wild-type BCR clusters (Fig. 2 E). Collectively, these results indicate that the interaction of the clustered BCRs with the lipid raft probe did not require signaling or the actin cytoskeleton but rather appeared to rely on an intrinsic property of the clustered BCR.

FRET between Igα-YFP and Lyn16-CFP correlates temporally and spatially with BCR activation

Previous studies using FRET confocal microscopy provided evidence that antigen binding from solution resulted in a

an encounter with an ICAM-1– and antigen-containing bilayer. A merged image of YFP and Ea and the relative FIs of YFP (red) and Ea (green) across the contact area of the merged image indicated by red lines (scale, 20 µm) are given. CH27 B cells were either untreated or pretreated with the Src family kinase inhibitor PP_2 (50 µm for 1 h at 37°C) or latrunculin B (10 µm for 30 min at 37°C). (B) Three-channel images (CFP, YFP, and FRET) of individual cells as performed in A were collected at 2-s intervals, and the FRET efficiency (Ea) was calculated as in Fig. 1 and described in Materials and methods. The mean Ea + SEM from six untreated cells, five PP2-treated cells, and six latrunculin B–treated cells is shown. (C) CFP, YFP, Ea, and merged images of J558L B cells expressing either the wild-type NIP-specific BCR ($Ig\alpha_{YY}/Ig\beta_{YY}$)-YFP or the mutant signaling-deficient BCR ($Ig\alpha_{YY\rightarrow FF}/Ig\beta_{YY\rightarrow FF}$)-YFP and Lyn16-CFP 1 min after the B cells encountered ICAM-1– and antigen-containing bilayers. Bars, 10 µm. The tyrosine to phenylalanine mutations in the ITAM of Igα/Igβ are indicated as asterisks in the BCR diagram (GFPs and BCR are not drawn to scale). (D and E) The number of BCR microclusters (D) and the FRET efficiency (Ea; E) were determined for single J558L cells expressing either the wild-type BCR or ITAM mutant BCR during time-lapse TIRF microscope imaging for 10 min after the cells contacted ICAM-1– and antigen-containing bilayers. The number of BCR clusters and FRET efficiencies were determined as described in Materials and methods at the time of peak FRET. Frequency plots of representative cells taken from the data of four independent experiments are shown. Horizontal lines are the median values of all individual points. D, 15–20 cells; E, 10–15 cells. P-values determined by *t* test are also shown.

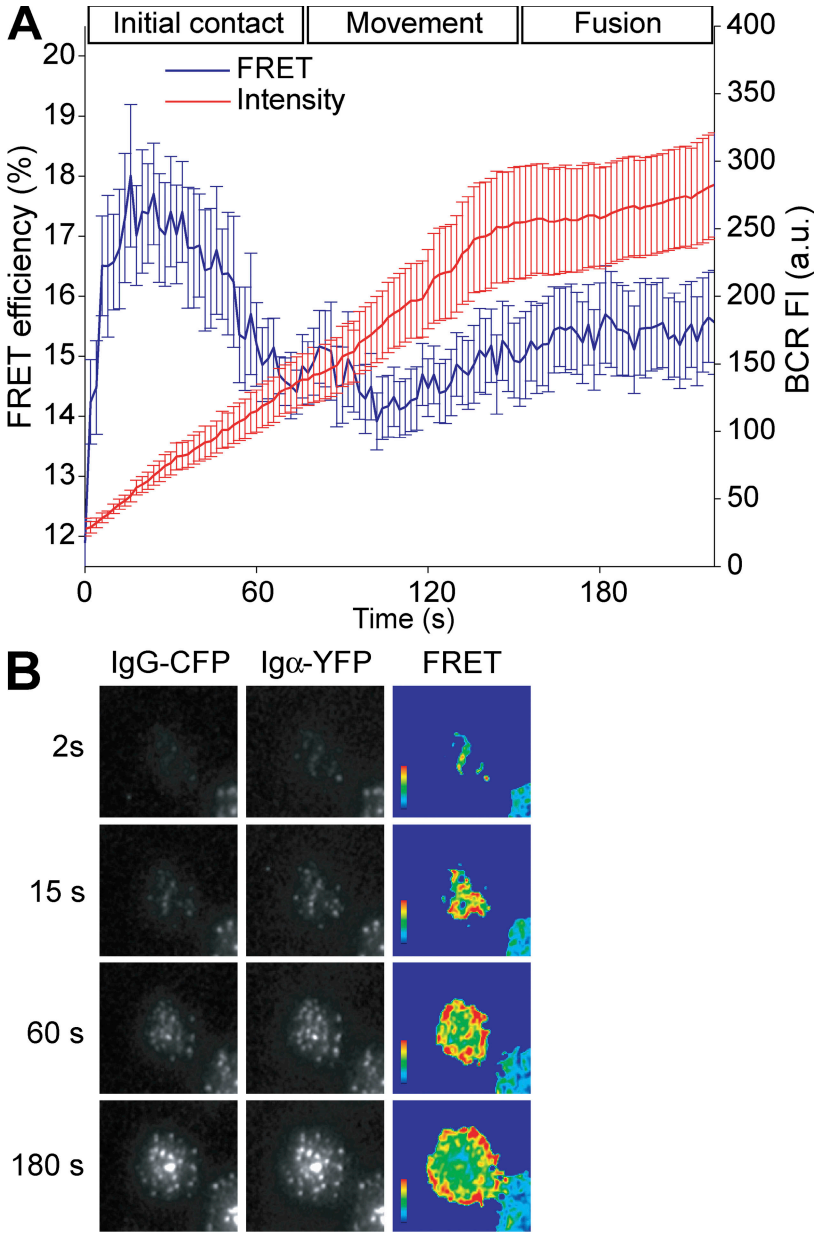

Figure 3. **Conformational change in the BCR cytoplasmic domains correlates temporally and spatially with the BCR's association with the lipid raft probe.** (A) J558L cells expressing B1-8γ-CFP and Igα-YFP were allowed to spread on bilayers containing NIP_{14}-BSA. TIRFM images were acquired, and FRET efficiency was calculated from tracking of individual clusters of the BCR as described in Materials and methods. Data represent mean ± SEM (error bars) from 14 clusters from multiple cells in four independent experiments. The corrected average FI of the BCR in clusters is also shown. Corresponding phases of the cluster lifetime are shown at the top. (B) Images of J558L cells expressing B1-8γ-CFP and Igα-YFP spreading on a NIP_{14}-BSA–containing bilayer. IgG-CFP (left) and YFP/CFP fluorescence ratio images at 442-nm laser illumination at the indicated times from the initial contact are shown.

conformational change in the BCR cytoplasmic domains from a "closed" to an "open" form and simultaneous phosphorylation of the BCR (Tolar et al., 2005). We observed that when clustered by antigen, BCRs containing a membrane Ig–CFP and Igα-YFP showed an initial increase in FRET, reflecting the close molecular proximity of the cytoplasmic domains of the clustered BCRs, and then a drop in FRET, indicating that the cytoplasmic domains within the BCR clusters moved apart or opened. To determine whether the observed FRET between Igα-YFP and Lyn16-CFP correlated either temporally or spatially with the antigen-induced transition in the BCR to an open form, we measured FRET in a J558L cell line expressing an NIP-specific BCR containing membrane Ig–CFP and Igα-YFP as the B cells encountered a bilayer containing NIP and ICAM-1 (Fig. 3). Tracking the initial BCR microclusters individually from their formation to the generation of the synapse showed that within the first few seconds of formation, FRET in the microclusters sharply increased, indicating the induced close molecular proximity of the cytoplasmic domains of the BCRs within the microclusters (Fig. 3 A). Despite the continued accumulation of BCRs in the clusters, the FRET level reached a peak and then dropped, which is consistent with a synchronized opening of the cytoplasmic domains of the BCR clusters as previously described (Tolar et al., 2005).

Calculation of FRET ratio images showed that the increase in FRET in the BCR clusters occurred in the initial point of contact and in the cell's periphery (Fig. 3 B). In contrast, the clustered BCRs accumulated in the synapse showed lower FRET, indicating an open conformation. Thus, transition of the BCR from the closed to open form correlated with FRET between Igα-YFP and Lyn16-CFP both spatially, occurring in the initial contact points and in the periphery of the B cell's contact area, and temporally, occurring within the first several seconds of encounter with the antigen bilayer.

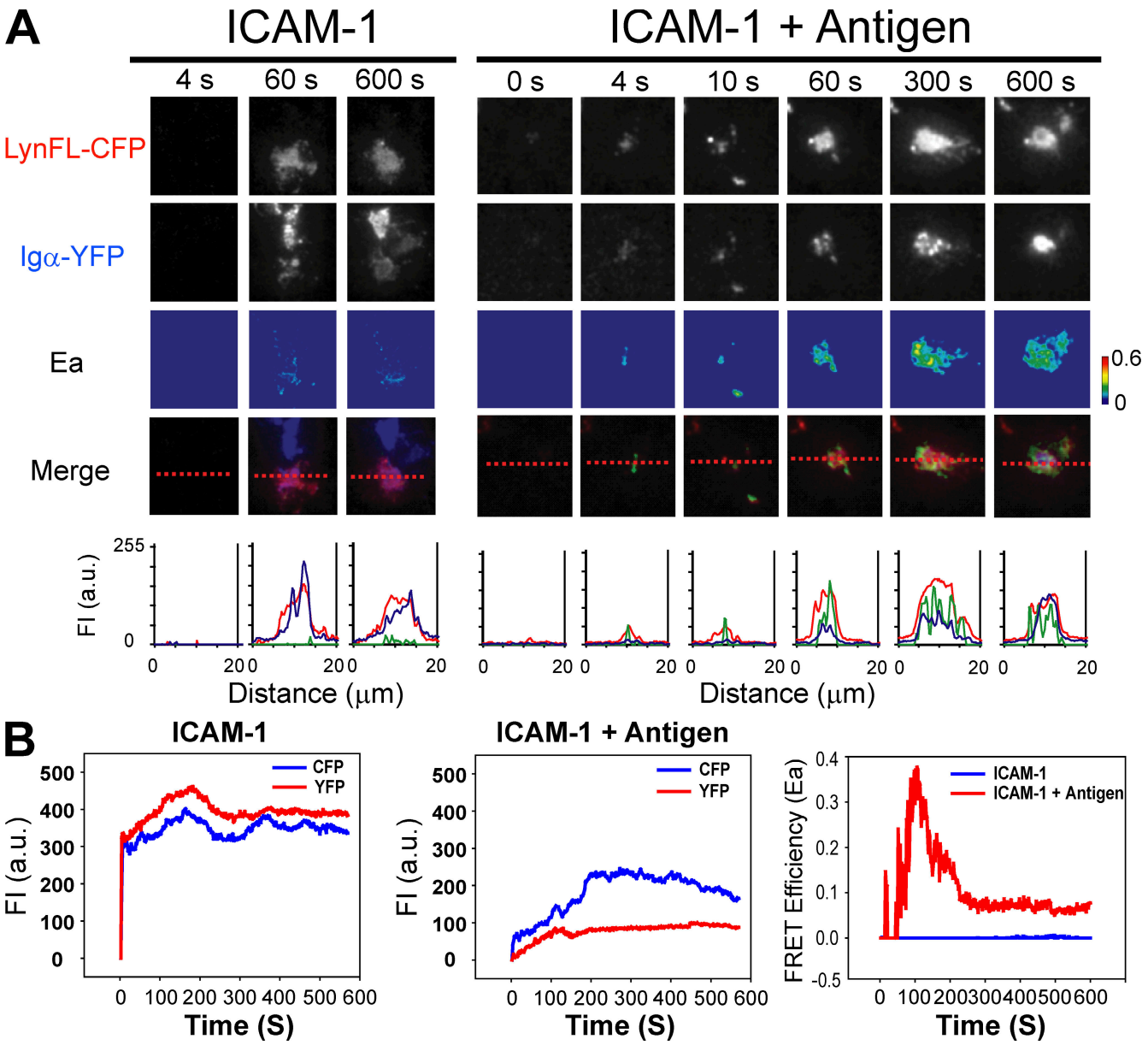

Figure 4. **The antigen-induced association of Lyn kinase with BCR.** (A) CFP, YFP, Ea, and merged time-lapse images of CH27 B cells expressing LynFL-CFP and Igα-YFP 0–600 s after the encounter of either ICAM-1 alone or ICAM-1– and antigen-containing bilayers. CFP and YFP FIs and Ea across the contact area indicated by red lines (scale, 20 μm) are given. (B) Quantification of the Igα-YFP and LynFL-CFP FIs and Ea plotted against time for cells imaged in A.

The antigen-induced interactions of the BCR with Lyn

Association of the antigen-induced BCR microclusters with the lipid raft probe has been suggested to play a role in facilitating the association of clustered BCR with the Lyn kinase. To directly characterize the interaction of the BCR with Lyn, CH27 B cells were analyzed that expressed Igα-YFP and full-length Lyn (LynFL) linked by six amino acids at the C terminus to CFP (LynFL-CFP). Images of B cells engaging a bilayer containing only ICAM-1 showed extensive colocalization of Igα-YFP with LynFL-CFP but no FRET (Fig. 4 A). In contrast, images of B cells engaging an ICAM-1– and antigen-containing bilayer showed significant FRET at the first points of contact where LynFL-CFP colocalized with Igα-YFP (Fig. 4 A). FRET between LynFL-CFP and Igα-YFP persisted as the BCR microclusters formed a central synapse. Quantification of the FIs and FRET over the contact area with time showed that although the relative FIs of Igα-YFP and LynFL-CFP were similar with time in the presence or absence of antigen, FRET was only detected when antigen was present (Fig. 4 B). Thus, the FRET cannot be attributed to a change in the ratios of YFP and CFP. The concentration of FRET between the BCR and LynFL in the center synapse was in contrast to the observation for the lipid raft probe and BCR, in which case FRET was highest in the cell's periphery. A time-lapse video illustrated this difference, showing that FRET between the BCR and raft lipid probe was more restricted to the cells' periphery in contrast to the FRET between Lyn and the BCR that was concentrated in the

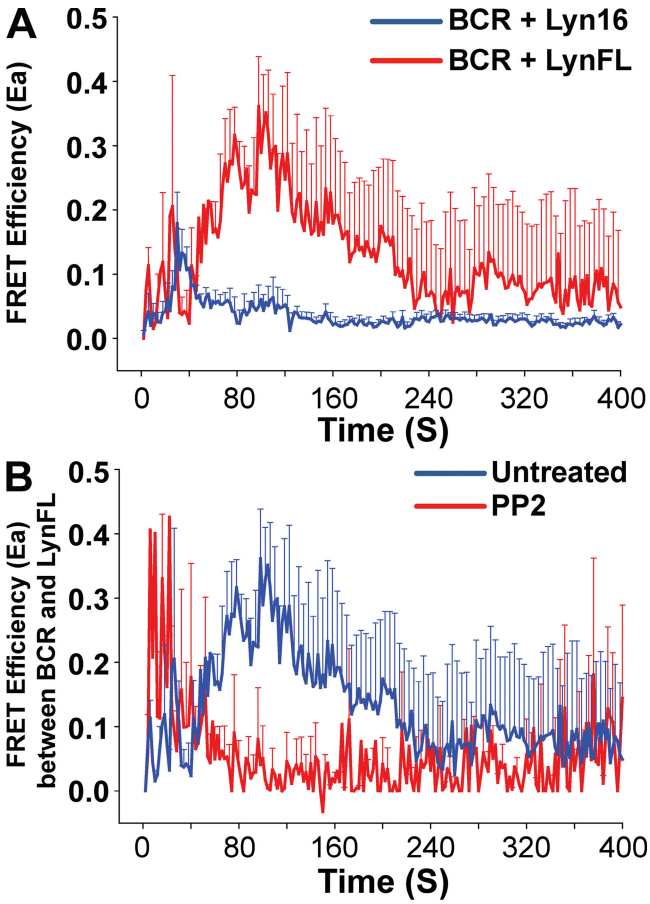

Figure 5. **FRET between antigen-clustered BCR and Lyn kinase is prolonged and sensitive to PP2 inhibition.** (A) Comparison of FRET efficiencies between Igα-YFP and Lyn16-CFP and between Igα-YFP and LynFL-CFP with time. (B) A comparison of the Ea between Igα-YFP and LynFL-CFP in the presence or absence of PP2. The calculation of FRET efficiency was performed as described in Materials and methods. Mean + SEM (error bars) of calculated Ea are shown with time for 12 cells expressing Lyn16-CFP, six cells expressing LynFL-CFP, and three cells expressing LynFL-CFP treated with PP2.

synapse (Fig. S1 and Videos 1–8, available at http://www.jcb.org/cgi/content/full/jcb.200802007/DC1).

FRET between Igα-YFP and either Lyn16-CFP or LynFL-CFP was quantified with time over the entire contact area of the B cells interacting with ICAM-1– and antigen-containing bilayers and was compared (Fig. 5 A). FRET between Lyn16-CFP and Igα-YFP increased rapidly upon initial B cell contact with the antigen-containing bilayer during the initial contact phase and then decreased as B cells spread and BCR clusters moved to the center of the synapse. FRET between LynFL-CFP and Igα-YFP showed an initial small peak that corresponded in time to the FRET between Igα-YFP and Lyn16-CFP during the initial contact phase (Fig. 5 A). The initial FRET peak between Igα-YFP and LynFL-CFP was followed by a peak in FRET that was significantly greater in magnitude and persisted for longer as the BCR clusters moved to the center of the synapse. Importantly, in cells treated with PP2 to block Lyn's activity, FRET between Igα-YFP and LynFL-CFP was limited to only the first peak in the initial contact phase (Fig. 5 B). Thus, Lyn appears to interact with the BCR clusters first in a PP2-resistant fashion, presumably mediated by lipid–protein interactions between Lyn and the BCR, and then in a PP2-sensitive phase, presumably by protein–protein interactions between the BCR and a kinase-active Lyn. Collectively, these observations indicate that over the contact area, BCR interactions with the lipid raft probe preceded those of the BCR and Lyn and that these lipid–protein interactions are more transient or unstable as compared with the protein–protein interactions between Lyn and the BCR.

Individual BCR microclusters associate with the lipid raft probe and with Lyn several seconds after forming

To better understand the dynamics between the formation of BCR microclusters and their association with Lyn and the lipid raft probe, we compared the pattern of FRET between either Lyn16-CFP or LynFL-CFP and Igα-YFP in individual BCR microclusters as the clusters first formed in membrane protrusions during the first 44 s of contact of the B cell with the antigen-containing bilayer (Fig. 6 A). BCR microclusters appeared ∼12–20 s before Lyn16-CFP colocalized with the BCR clusters and FRET between Lyn16-CFP and Igα-YFP was detected (Fig. 6 A). In these microclusters, the FRET appeared to increase, peak, and then decrease. Similarly, BCR clusters were detected and colocalized with LynFL-CFP ∼20–28 s before FRET was detected at 28–44 s (Fig. 6 A). Thus, BCR clustering preceded by several seconds the close molecular association of BCR with the lipid raft probe and with Lyn. In addition, these results showed no evidence that the lipid raft probes and Lyn are in preformed structures, but rather both appeared to coalesce around the BCR microclusters.

Association of the BCR with Lyn facilitates directional movement to the synapse

It was of interest to determine the repercussions of the association of the BCR microclusters with the lipid raft probe as compared with Lyn itself in terms of the movement of the microclusters from the cell's periphery to the cell's center to form an immune synapse. To do so, the trajectories of individual BCR microclusters were analyzed as they formed in the periphery and moved to the synapse to determine when microclusters associated with the raft probe versus Lyn (Fig. S2 and Video 9, available at http://www.jcb.org/cgi/content/full/jcb.200802007/DC1). The trajectories of the BCR clusters formed in the periphery of the contact area showed three patterns: an immediate movement toward the center of the contact area, a delayed movement to the center, and a random nondirectional movement in the periphery. FRET between BCR clusters and the lipid raft probe or Lyn was measured in cells expressing either Igα-YFP and Lyn16-CFP or Igα-YFP and LynFL-CFP. An analysis of the time the BCR clusters moved randomly before moving in a directed trajectory to the center of the contact area showed that the clusters associated with Lyn16-CFP spent considerably more time in a random movement (an average of 25 s) before moving to the center as compared with those associated with LynFL-CFP (an average of 8 s; Fig. 6 B). This observation suggests that association of the BCR with Lyn facilitates directional movement to the synapse.

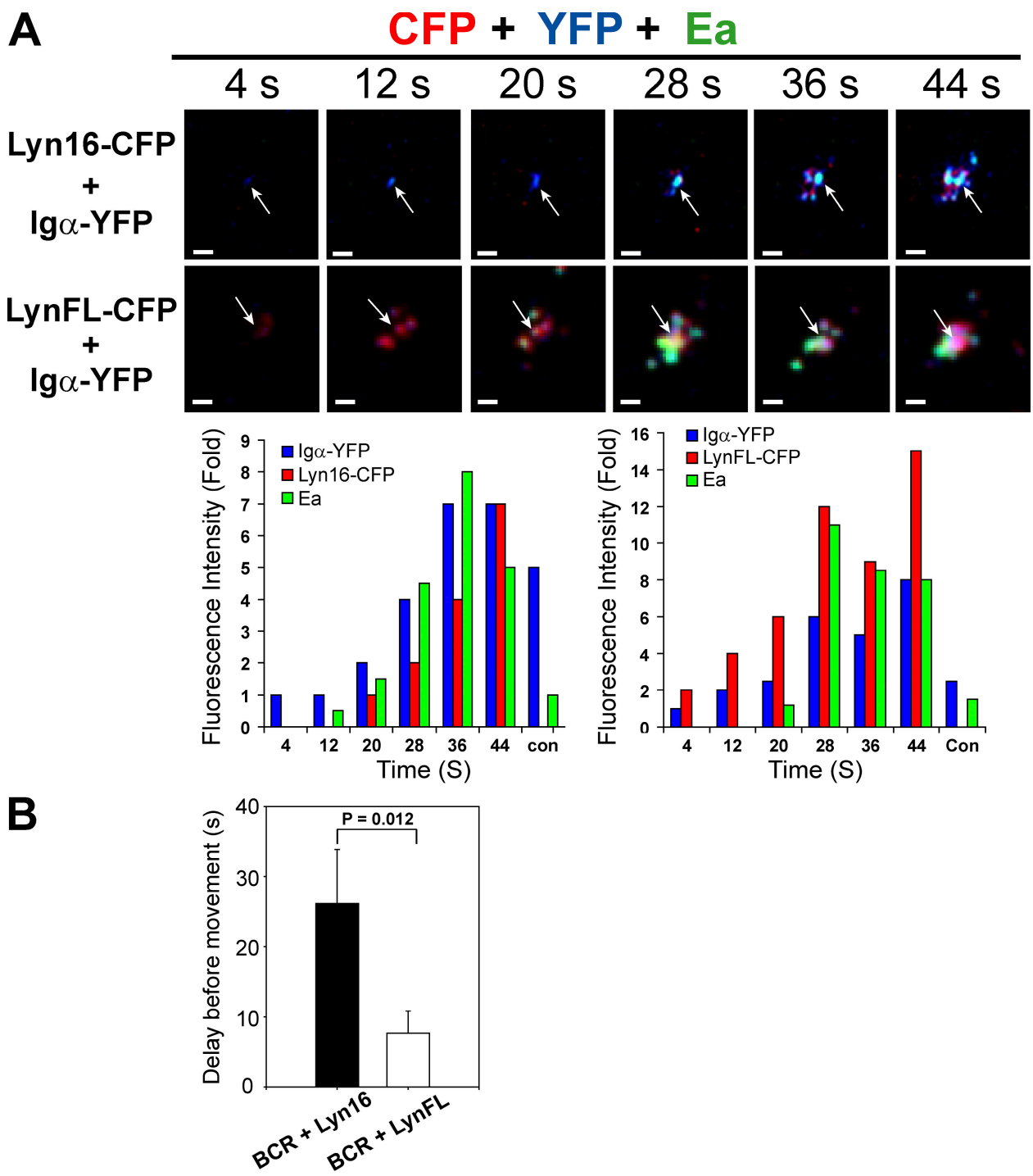

Figure 6. **BCR clustering precedes by several seconds the association of clustered BCR with raft lipids and Lyn kinase.** (A) The merged TIRFM images of CFP (red), YFP (blue), and Ea (green; top) and quantification of the fold increases of CFP and YFP FIs and Ea for the BCR microclusters (bottom). The images were taken at 8-s intervals of CH27 B cells expressing either Igα-YFP and the lipid raft probe, Lyn16-CFP (top row), or Igα-YFP and LynFL kinase, LynFL-CFP (bottom row), as the cell first encounters an ICAM-1– and antigen-containing bilayer. The clusters marked by white arrows were quantified as the fold intensities relative to the intensities of the first frame in each channel showing a signal over background over a 4-μm^2 region of interest surrounding the clusters. Bars, 2 μm. (B) TIRFM time-lapse images were taken of CH27 B cells expressing either Igα-YFP and Lyn16-CFP or Igα-YFP and LynFL-CFP as they contacted PC_{10}-BSA– and ICAM-1–containing bilayers. Individual BCR clusters that formed in the periphery of the contact area and moved to the central synapse were tracked, and the pattern of movement of single BCR clusters was analyzed by time-lapse Ea images as described in Materials and methods. The time delay before a cluster that formed in the periphery moved to the center was determined. A total of ~200 clusters from cells expressing either both Igα-YFP and Lyn16-CFP (four cells) or both Igα-YFP and LynFL-CFP (three cells) were included in the analyses. Error bars represent SEM.

Discussion

The use of live cell imaging allowed an investigation into the earliest events in the initiation of BCR signaling that precede the interaction of the BCR with Lyn kinase and the formation of an immunological synapse (Fig. S3, available at http://www.jcb.org/cgi/content/full/jcb.200802007/DC1). We provide evidence for an ordered series of events that begins with the antigen-induced clustering of the BCRs. The newly clustered BCRs associate with a lipid raft probe in the periphery of the contact area of the B cell with an antigen-containing lipid bilayer. Association of the antigen-clustered BCRs with the lipid raft probe is highest in the cells' periphery and weaker as the BCR clusters move to the center of the contact area to form a synapse. BCR clusters associated with a lipid raft probe appear to move randomly in the peripheral contact area, and it is not until the clustered BCRs stably associate with Lyn that the random motion ceases and the BCR clusters move directionally to the center of the contact area to form a synapse.

In interpreting FRET data generated using intermolecular reporters, as described here, it is important to control for potential artifacts that can result from relative differences in the concentrations of the two reporters. The influence of the concentration on artifacts in the FRET measurements can largely be avoided by calibrating the bleed-through of the donor fluorescence in the acceptor detection channel and the amount of directly excited acceptor fluorescence as described previously (van Rheenen et al., 2004; Zal and Gascoigne, 2004). In the studies reported here, calibration involved the use of control cells in the same field as the experimental cells, that each contained only the acceptor or the donor fluorescent protein and measurements at the donor and acceptor emission wavelengths. Nevertheless, it is possible that an effect of the changes in concentration of the BCR as it clusters was directly responsible for the changes in measured FRET. We have addressed this issue by providing data demonstrating that although the ratio of FIs of the CFP and YFP did not change significantly over time on cells engaging bilayers containing ICAM alone or ICAM plus the antigen, FRET was only observed in cells engaging antigen. Moreover, the spatial pattern of FRET did not correlate with the highest intensities of YFP and CFP, a correlation that should occur if FRET was simply the result of the concentration of the clustered BCR. We also provided data demonstrating that FRET between Igα-YFP and Lyn16-CFP was specific and did not occur between Igα-YFP and a different lipid probe, namely geranylgeranyl-CFP, even though the FIs were similar in both cases for CFP and YFP. Collectively, these results provide strong evidence that the FRET measurements reported here reflect a genuine, specific molecular interaction between Igα-CFP and Lyn16-YFP and LynFL-YFP.

The view of lipid rafts and their interactions with immune receptors during antigen engagement provided by these studies differ in the molecular details from earlier views as first articulated in the raft hypothesis (Simons and Ikonen, 1997). Lipid rafts were initially viewed as freely diffusing, stable, lateral assemblies of sphingolipids and cholesterol that formed signaling platforms. In the intervening years, results of studies of both model membranes and living cells along with computational modeling led to an updated model of lipid rafts that takes into account a more dominant role for membrane proteins in capturing and stabilizing intrinsically unstable liquid-ordered membrane microdomains (Hancock, 2006). Here, we provide evidence consistent with this updated version of the raft hypothesis. The raft lipids do not appear to form stable microscopic structures either in resting or activated cells. Indeed, we were unable to detect FRET between Lyn16-YFP and Lyn16-CFP in cells that expressed both (unpublished data), suggesting that stable raft microdomains, if they exist, must be small as indicated previously (Sharma et al., 2004). Second, the results provided here indicate that the BCRs first cluster and then condense raft lipids around them. These clustered BCR–raft lipid interactions are dynamic, weak, and transient. The interaction of lipid rafts with the clustered BCRs is not dependent on the initiation of signaling or on the actin cytoskeleton and thus appears to be an intrinsic property of the clustered BCR that prefers the microenvironment of raft lipids.

In contrast to the ephemeral interactions of the clustered BCRs with raft lipids that predominate early after BCR clustering, the BCR forms more stable protein–protein interactions with Lyn that dominate later and are dependent on a kinase-active Lyn. Indeed, association of the clustered BCR with Lyn predicted the directional movement of the BCRs to the synapse. These observations are similar to those of Larson et al. (2005), who showed that LynFL codiffuses with the clustered IgE receptor, but a minimal raft probe did not. Similarly, Douglass and Vale (2005) used TIRFM to observe the diffusion of single molecules on the surface of T cells during T cell activation by antigen and provided evidence for membrane microdomains created by protein–protein networks that exclude or trap signaling molecules on the T cells' membrane. They provided evidence that the full-length Src family kinase, Lck, stably associated with T cell receptor signaling domains, but the minimal lipid probe did not. However, these domains were large and formed relatively late after antigen engagement, and the authors suggested that lipid raft–receptor interactions might precede the formation of these domains and play an organizational role within a receptor cluster. Here, we provide evidence that this may indeed be the case for signaling through the BCR. Collectively, these studies illustrate the importance of both lipid–protein and protein–protein interactions in the initiation of signaling.

The results presented here characterizing the interaction of BCR microclusters and a lipid raft probe during contact of the B cell with antigen on a membrane differ from our previous results characterizing the same process in B cells responding to antigen in solution (Sohn et al., 2006). In response to soluble antigen, BCR–lipid raft probe interactions were blocked by PP2, a Src family kinase inhibitor (Sohn et al., 2006). In contrast, we show here that in response to antigen on membranes, PP2 does not block interactions of the BCR with the lipid raft probe, although PP2 influences the dynamics of the interactions. In addition, we show here that a signaling-deficient BCR associates with the lipid raft probe upon clustering in response to membrane-bound antigen. These findings raise the question of how the B cells' encounter with antigens on membrane differs from that with antigen in solution. When interacting with antigens on membranes, the topology of the B cell membrane changes dramatically.

The initial contacts are through small membrane protrusions that may concentrate or restrict BCR movement, facilitating clustering. These interactions trigger spreading of the BCR over the antigen-membrane and then contraction. It may be that Src kinase activity is required for B cells in solution to provide a restriction on BCR membrane movements that is replaced or overcome by membrane topology in B cells encountering membrane-bound antigens. Clearly, additional studies will be required to fully delineate the mechanisms at play in these early events.

The observation that BCR clusters associate with lipid rafts raises the following question: what function do lipid rafts provide? Using FRET confocal microscopy, we previously showed that the cytoplasmic domains of antigen-clustered BCRs undergo a conformational change from a closed to an open form (Tolar et al., 2005). We show here that the transition of the clustered BCR from the closed to an open form correlates both temporally and spatially with condensing of the raft lipid probe around the clustered BCR. By several criteria, the open form of the BCR was signaling active and phosphorylated by Lyn. We speculate that the well-characterized local thickening of raft membranes (McIntosh et al., 2003) or the curvature of the raft membrane (Reynwar et al., 2007) around the clustered BCR may induce the observed conformational change in the clustered BCR cytoplasmic domains. The open BCR cluster would then be phosphorylated by Lyn that was also condensed around the clustered BCR by virtue of its lipid anchor to the plasma membrane. Thus, lipid rafts may provide two distinct functions: namely, to segregate the BCR and Lyn in the plane of the membrane in resting cells and facilitate their interactions after BCR clustering and to alter the character of the membrane surrounding the clustered BCR, inducing an alteration in the conformation of the cluster to accommodate the membrane change. Thus, interaction of the BCR with membrane lipids may play a critical role in the initiation of signaling.

Materials and methods

Cell lines, antigens, and reagents

The CH27 mouse B cells that stably express the recombinant chimeric protein Igα-YFP (Igα fused to the N terminus of YFP) alone or Igα-YFP and Lyn16-CFP (containing the first 16 amino acids of Lyn, including the myristoylation and palmitoylation sequences on the N terminus of the monomeric form of CFP) were described previously (Sohn et al., 2006). The J558L B cell line, which stably expresses the NIP-specific B1-8 μ heavy chain, was maintained as previously described (Tolar et al., 2005). PC conjugated with BSA containing 10 PC per BSA (PC_{10}-BSA; Biosearch Technologies) was used as an antigen for the PC-specific CH27 cell line, and NIP_{16}- or NIP_{14}-BSA containing 16 or 14 NIP groups per BSA molecule (Dal Porto et al., 1998) was used as the antigen for the NIP-specific J558L cell line. PP2 and latrunculin B were purchased from EMD, and 50 μM PP2 and 10 μM latrunculin B were used in the experiments as needed.

Constructs and transfection

The LynFL-CFP construct was generated by inserting an XhoI–BamHI fragment containing LynFL (provided by B. Baird, Cornell University, Ithaca, NY; Kovarova et al., 2001; Hess et al., 2003) into the pECFP-N1 vector (Clontech Laboratories, Inc.). The monomeric form of geranylgenaylated CFP (Ger-CFP) construct was generated by PCR primer extension using 5′ primer encoding the N terminus of CFP and 3′ primer encoding the C terminus of CFP with an additional 16 amino acids (DGKKKKKKSKTKCQLL), including the C-terminal polybasic12 residues of K-ras and four residues of rap1B, resulting in geranylgeranylation of the expressed proteins (Pyenta et al., 2001), and a monomeric CFP-expressing plasmid as a template. The PCR product was inserted to the pECFP-N1 vector and confirmed sequences for the construct. CH27 cells were generated that expressed either both the LynFL conjugated to the N terminus of the monomeric version of CFP (LynFL-CFP) and Igα-YFP or both Ger-CFP and Igα-YFP. J558L cells stably transfected with wild-type $Ig\alpha_{YY}$ (Tolar et al., 2005) were transiently transfected with wild-type $Ig\beta_{YY}$-YFP and Lyn16-CFP. J558L cells stably transfected with the mutant $Ig\alpha_{YY\rightarrow FF}$ (Tolar et al., 2005) were transiently transfected with Lyn16-CFP and mutant $Ig\beta_{YY\rightarrow FF}$-YFP.

Planar lipid bilayers

The preparation of planar lipid bilayers is detailed elsewhere (Grakoui et al., 1999; Carrasco et al., 2004). Bilayers were prepared that contained biotin lipids to which biotinylated ICAM-1 and antigens were attached through streptavidin. In brief, PC_{10}-BSA, NIP_{16}-BSA, and the mouse ICAM-1/huFc chimera protein (R&D Systems) were biotinylated with EZ-link sulfo-NHS-LC-biotin (Thermo Fisher Scientific). An aliquot of each was labeled with sulfo-NHS–functionalized fluorophores (Invitrogen) to allow monitoring of the mobility of the lipid-anchored proteins in the lipid bilayers. Biotin-labeled small unilamellar lipid vesicles were prepared by mixing a 100:1 molar ratio of 1,2-dioleoyl-*sn*-glycero-3-phosphocholine and 1,2-dioleoyl-*sn*-glycero-3-phosphoethanolamine-cap-biotin (Avanti Polar Lipids, Inc.). The lipid mixture was sonicated and resuspended in PBS at a lipid concentration of 5 mM. Aggregated lipid vesicles were cleared by ultracentrifugation and filtering.

Bilayers were formed in Lab-Tek chambers (Thermo Fisher Scientific) in which the coverglasses were replaced with nanostrip-washed coverslips. The coverslips were incubated with 0.1 mM biotin-labeled small unilamellar lipid vesicles in PBS for 10 min. After washing with 20 ml PBS, the bilayer was incubated with 2.5 μg/ml streptavidin for 10 min, and excess streptavidin was removed by washing with 20 ml PBS. The bilayers were incubated for 20 min with 0.5 μg/ml of biotinylated mouse ICAM-1, and excess ICAM-1 was removed by washing. The streptavidin- and ICAM-1–containing planar lipid bilayers were incubated with 0.75 μg/ml of biotinylated PC-BSA or NIP-BSA. The unbound excess of antigen was removed by washing with 20 ml PBS. The mobility of ICAM-1 and antigens in the lipid bilayers was confirmed by analyses of the proteins labeled with fluorescent dyes.

Alternatively, NIP- and ICAM-1–containing planar lipid bilayers were prepared by fusing small unilamellar lipid vesicles with a clean glass coverslip surface as described previously (Brian and McConnell, 1984) using 1,2-dioleoyl-*sn*-glycero-3-phosphocholine and 1,2-dioleoyl-*sn*-glycero-3-[*N*-(5-amino-1-carboxypentyl iminodiacetic acid) succinyl] in nickel salt (Avanti Polar Lipids, Inc.) at a 10:1 ratio. Small unilamellar vesicles were obtained by sonication and clarified by ultracentrifugation and filtering. Glass coverslips were cleaned in Nanostrip (Cyantek), washed, and dried. Lipid bilayers were prepared from a 0.1-mM lipid solution on the coverslips attached to the bottom of Lab-Tek imaging chambers. After excess lipids were washed away, histidine-tagged antigens and ICAM-1 were bound. Before imaging, chambers were washed with HBSS supplemented with 1% FCS. NIP_{14}-BSA was prepared as described previously (Tolar et al., 2005) and conjugated to a cystein-containing peptide terminated with a 12-histidine tag (ASTGTASACTSGASSTGSH_{12}) using SMCC (Thermo Fisher Scientific) according to the manufacturer's protocols. Recombinant ICAM-1 tagged with a 12-histidine tag was a gift from J. Huppa (Stanford University, Palo Alto, CA). Conjugation of NIP_{14}-BSA to succinimidyl AlexaFluor647 and ICAM-1-H12 to AlexaFluor488 (both obtained from Invitrogen) was performed according to the manufacturer's protocols.

TIRFM imaging and image analysis

Through-lens TIRFM (Axelrod, 1981) was performed on an inverted microscope (IX-81; Olympus) equipped with 60× 1.45 NA and 100× 1.45 NA objectives (Olympus). For Figs. 1 C and 5 A, 100× 1.45 NA objectives were used for the image acquisition. Cells expressing CFP and/or YFP were added onto the lipid bilayers containing ligands, and all time-lapse imaging was performed at 37°C using a heated chamber. A 442-nm laser (Melles Griot) was used for CFP excitation, and CFP and FRET images were acquired simultaneously using a dual image splitter (MAGS Biosystems) equipped with a 505 dichroic beamsplitter and HQ485/30 (CFP) and HQ560/50 (FRET) emission filters (Chroma Technology Corp.). The 514-nm line from an argon gas laser was used to excite YFP, and images were acquired through the same dual image splitter with the HQ560/50 filter. CFP-FRET and YFP dual-view images were sequentially acquired in each time point through the alternative switch of each laser line.

Images were captured into 16-bit grayscale with no binning and no averaging as 512 × 512 pixels by an electron-multiplier charge-coupled device camera (Cascade II; Photometrics) under management by MetaMorph software (MDS Analytical Technologies). Otherwise, a 1,024 × 1,024–pixel size of images recorded into 10-bit grayscale with an intensifier

CCD camera (XR/MEGA-10; Stanford Photonics) was obtained under control by QED software (Media Cybernetics, Inc.) for Figs. 6 A (top row) and S2.

FRET images obtained by TIRFM were analyzed by the sensitized acceptor emission method as described in detail previously (van Rheenen et al., 2004; Tolar et al., 2005; Sohn et al., 2006). The FRET efficiency normalized for the acceptor (Ea) predominantly used here was described in a previous paper in detail (Tolar et al., 2005). In brief, first, three CFP (D), FRET (F), and YFP (A) images were obtained by splitting CFP-FRET and YFP dual-view images into each CFP, FRET, and YFP image after alignment between two images using the custom-made macro function in the Image Pro Plus software package (Media Cybernetics, Inc.). CFP-FRET dual-view images from 1.0 µm of blue-green fluorescent polystyrene microspheres (excitation/emission of 430/465) that fluoresce in both the CFP and FRET channels (Invitrogen) were used as an alignment reference in each experiment. Second, the CFP, FRET, and YFP images were background subtracted, flattened for background, and smoothed by a Gauss filter method using Image Pro Plus software. FRET efficiency (Ea) was calculated by the following equation: $Ea = (F - \beta \times D - \gamma \times A)/\gamma \times A \times K_A$ as described previously (Tolar et al., 2005). Correction factors for donor (CFP) bleed-through (β) and acceptor (YFP) cross talk (γ) in the FRET channel were obtained from single CFP- or YFP-expressing cells present in the same image fields with the experimental cells to eliminate the bias among different fields or times. The β factor was 0.7 ± 0.05, and the γ factor was 0.6 ± 0.1. In our TIRF microscope system, the bleed-through of YFP emission in FRET channel to the CFP channel during 442-nm excitation (δ factor) from the YFP single positive cell was negligible. The K_A constant was obtained as described previously (Tolar et al., 2005) by acquiring TIRF as well as epifluorescence images of Daudi, human B cells expressing Lyn16-CFP-YFP fusion proteins (Sohn et al., 2006). The $E_{bleaching}$ value from the control cells was mainly obtained from the epifluorescence images before and after bleaching YFP because of the ease of bleaching. The $E_{bleaching}$ and K_A values were 0.5 ± 0.5 and 5 ± 0.2, respectively, in our setting condition.

For the quantification of FRET at the single-cell level with time, the mean FIs from the background-subtracted images of each CFP, FRET, and YFP channel were calculated from a region of interest over background levels using the autotracking mode of Image Pro Plus software. FRET efficiencies (Ea) were calculated by the aforementioned equation, and data are shown as the mean ± SEM. For counting the number of BCR microclusters per cell in Fig. 2 D, YFP-probed IgM clusters that appeared on the TIRF images were manually counted in each cell after bandpass filtering the images using Matlab software (The Mathworks, Inc.). FRET between BCR subunits in Fig. 3, in which the stoichiometry of donor and acceptor is constant, was calculated only from CFP and FRET images as

$$E = \frac{R - \beta - \frac{K_D}{nK_A}}{R - \beta + K_D},$$

where R is the FRET/CFP fluorescence ratio and n is the CFP:YFP stoichiometry ($n = 2$). FI of the BCR was calculated as $I = CFP/1 - E$. For image figures, all images shown were converted to the eight-bit scale from original 10- or 16-bit grayscale recorded in the nonsaturated level.

Single-particle–tracking analysis from time-lapse TIRF images

The time delay before movement of single BCR clusters associated with the lipid raft probe or with the Lyn in Fig. 6 B or in Fig. S2 was analyzed. Time-lapse TIRFM FRET images were acquired as described in the previous section from CH27 cells expressing either Igα-YFP and Lyn16-CFP or Igα-YFP and LynFL-CFP. The images were analyzed by single-particle tracking using Image Pro Plus software. Tracking was performed by autotracking particles determined by centroid analysis above 0.5 μm^2 that moved within a distance of 1 µm at each time interval with one image frame skip. Clusters that merged or split were included in the tracking analysis. To eliminate artifacts of autotracking, the analyses were manually confirmed. About 200 particles from three to four cells were analyzed, and *t* tests were used to determine the significance of the differences between Igα-YFP-Lyn16-CFP clusters and Igα-YFP-LynFL-CFP clusters. The confinement index (Schwickert et al., 2007) was calculated as the ratio of the original distance traveled to the accumulated distance and was used as a criteria for the classification of particle movements: >0.8, directional; 0.4–0.8, delayed directional; <0.4, random. When a cluster transitioned from random to directional movement, the time spent in random movement was calculated and expressed as the time delay. For Video 9, Igα-YFP clusters were tracked using the following custom macros. In brief, the BCR clusters were first bandpass filtered and, clusters above a selected threshold were chosen for single-cluster tracking using custom-made Matlab script. Single-cluster tracking was performed at the same settings used in Image Pro Plus software analysis (Figs. 6 B and S2) with the exception that the Gaussian-fitted position of the clusters was determined using Matlab script. In all cases, the accuracy of the tracking algorithm was checked visually, and, when needed, the algorithm parameters were adjusted to provide optimal tracking. Cluster trajectories >100 s during the contraction phase were used. The track of each cluster was confirmed manually. Several representative BCR clusters showing directional (Video 9, red circles), delayed directional (Video 9, green circles), and random (Video 9, blue circles) movements were color assigned, and the video was made at 10 frames per second using Matlab script. For calculation of the average molar ratio of YFP to CFP over the contact area of cells to the lipid bilayer, CFP and YFP FIs were obtained at each time point and compared with the CFP and YFP FIs obtained from Daudi B cells expressing Lyn16-mCFP-YFP fusion protein given a 1:1 molar ratio as a reference. In reference cells, CFP intensity was obtained after YFP photobleaching. In our setting, a 1:1 ratio of CFP and YFP FIs gives a 10:1 molar ratio.

Online supplemental material

Fig. S1 shows that the association of antigen-clustered BCR with raft lipid probe differs from that with Lyn kinase dramatically using time-lapse images. Fig. S2 shows the dynamic movement of BCR clusters as they associate with raft lipids and move to the synapse using single-cluster tracking. Fig. S3 shows a model for the role of raft lipids in B cell activation. Videos 1–8 are the videos from which the eight still images shown in Fig. S1 were taken. Video 9 shows the dynamic movement of BCR clusters to the synapse during the contraction phase after antigen binding on the lipid bilayer. Online supplemental material is available at http://www.jcb.org/cgi/content/full/jcb.200802007/DC1.

We thank B. Baird for providing Lyn-GFP constructs and J. Brzostowski for help with TIRFM.

This research was supported by the Intramural Research Program of the National Institute of Allergy and Infectious Diseases (National Institutes of Health).

Submitted: 1 February 2008
Accepted: 9 June 2008

References

Aman, M.J., and K.S. Ravichandran. 2000. A requirement for lipid rafts in B cell receptor induced Ca^{2+} flux. *Curr. Biol.* 10:393–396.

Axelrod, D. 1981. Cell-substrate contacts illuminated by total internal reflection fluorescence. *J. Cell Biol.* 89:141–145.

Batista, F.D., D. Iber, and M.S. Neuberger. 2001. B cells acquire antigen from target cells after synapse formation. *Nature.* 411:489–494.

Brian, A.A., and H.M. McConnell. 1984. Allogeneic stimulation of cytotoxic T cells by supported planar membranes. *Proc. Natl. Acad. Sci. USA.* 81:6159–6163.

Brown, B.K., and W. Song. 2001. The actin cytoskeleton is required for the trafficking of the B cell antigen receptor to the late endosomes. *Traffic.* 2:414–427.

Cambier, J.C., C.M. Pleiman, and M.R. Clark. 1994. Signal transduction by the B cell antigen receptor and its coreceptors. *Annu. Rev. Immunol.* 12:457–486.

Carrasco, Y.R., and F.D. Batista. 2006. B-cell activation by membrane-bound antigens is facilitated by the interaction of VLA-4 with VCAM-1. *EMBO J.* 25:889–899.

Carrasco, Y.R., S.J. Fleire, T. Cameron, M.L. Dustin, and F.D. Batista. 2004. LFA-1/ICAM-1 interaction lowers the threshold of B cell activation by facilitating B cell adhesion and synapse formation. *Immunity.* 20:589–599.

Cheng, P.C., M.L. Dykstra, R.N. Mitchell, and S.K. Pierce. 1999. A role for lipid rafts in B cell antigen receptor signaling and antigen targeting. *J. Exp. Med.* 190:1549–1560.

Dal Porto, J.M., A.M. Haberman, M.J. Shlomchik, and G. Kelsoe. 1998. Antigen drives very low affinity B cells to become plasmacytes and enter germinal centers. *J. Immunol.* 161:5373–5381.

Dal Porto, J.M., S.B. Gauld, K.T. Merrell, D. Mills, A.E. Pugh-Bernard, and J. Cambier. 2004. B cell antigen receptor signaling 101. *Mol. Immunol.* 41:599–613.

Depoil, D., S. Fleire, B.L. Treanor, M. Weber, N.E. Harwood, K.L. Marchbank, V.L.J. Tybulewicz, and F.D. Batista. 2008. CD19 is essential for B cell activation by promoting B cell receptor-antigen microcluster formation in response to membrane-bound ligand. *Nat. Immunol.* 9:63–72.

Douglass, A.D., and R.D. Vale. 2005. Single-molecule microscopy reveals plasma membrane microdomains created by protein-protein networks that exclude or trap signaling molecules in T cells. *Cell.* 121:937–950.

Edidin, M. 2003. The state of lipid rafts: from model membranes to cells. *Annu. Rev. Biophys. Biomol. Struct.* 32:257–283.

Fleire, S.J., J.P. Goldman, Y.R. Carrasco, M. Weber, F.D. Bray, and F.D. Batista. 2006. B cell ligand discrimination through a spreading and contraction response. *Science.* 312:738–741.

Grakoui, A., S.K. Bromley, C. Sumen, M.M. Davis, A.S. Shaw, P.M. Allen, and M.L. Dustin. 1999. The immunological synapse: a molecular machine controlling T cell activation. *Science.* 285:221–227.

Guo, B., R.M. Kato, M. Garcia-Lloret, M.I. Wahl, and D.J. Rawlings. 2000. Engagement of the human pre-B cell receptor generates a lipid raft-dependent calcium signaling complex. *Immunity.* 13:243–253.

Hancock, J.F. 2006. Lipid rafts: contentious only from simplistic standpoints. *Nat. Rev. Mol. Cell Biol.* 7:456–462.

Hanke, J.H., J.P. Gardner, R.I. Dow, P.S. Changelian, W.H. Brissette, E.J. Weringer, B.A. Pollok, and P.A. Connolley. 1996. Discovery of a novel, potent and Src family-selective tyrosine kinase inhibitor. *J. Biol. Chem.* 271:695–701.

Hess, S.T., E.D. Sheets, A. Wagenknecht-Wiesner, and A.A. Heikal. 2003. Quantitative analysis of the fluorescence properties of intrinsically fluorescent proteins in living cells. *Biophys. J.* 85:2566–2580.

Hou, P., E. Araujo, T. Zhao, M. Zhang, D. Massenburg, M. Veselits, C. Doyle, A.R. Dinner, and M.R. Clark. 2006. B cell antigen receptor signaling and internalization are mutually exclusive events. *PLoS Biol.* 4:e200.

Kovarova, M., P. Tolar, R. Arudchandran, L. Draberova, J. Rivera, and P. Draber. 2001. Structure-function analysis of lyn kinase association with lipid rafts and initiation of early signaling events after Fcε receptor I aggregation. *Mol. Cell. Biol.* 21:8318–8328.

Larson, D.R., J.A. Gosse, D.A. Holowka, B.A. Baird, and W.W. Webb. 2005. Temporally resolved interactions between antigen-stimulated IgE receptors and Lyn kinase on living cells. *J. Cell Biol.* 171:527–536.

McIntosh, T.J., A. Vidal, and S.A. Simon. 2003. Sorting of lipids and transmembrane peptides between detergent-soluble bilayers and detergent-resistant rafts. *Biophys. J.* 85:1656–1666.

Pyenta, P.S., D. Holowka, and B. Baird. 2001. Cross-correlation analysis of inner-leaflet-anchored green fluorescent protein co-redistributed with IgE receptors and outer leaflet lipid raft components. *Biophys. J.* 80:2120–2132.

Qi, H., J.G. Egen, A.Y.C. Huang, and R. Germain. 2006. Extrafollicular activation of lymph node B cells by antigen-bearing dendritic cells. *Science.* 312:1672–1676.

Reth, M., and J. Wienands. 1997. Initiation and processing of the signals from the B cell antigen receptor. *Annu. Rev. Immunol.* 15:453–479.

Reynwar, B.J., G. Illya, V.A. Harmandaris, M.M. Muller, K. Kremer, and M. Deserno. 2007. Aggregation and vesiculation of membrane proteins by curvature-mediated interactions. *Nature.* 447:461–464.

Schwickert, T.A., R.L. Lindquist, G. Shakhar, G. Livshits, D. Skokos, M.H. Kosco-Vilbois, M.L. Dustin, and M.C. Nussenzweig. 2007. In vivo imaging of germinal centres reveals a dynamic open structure. *Nature.* 446:83–87.

Sharma, P., R. Varma, R.C. Sarasij, Ira, K. Gousset, G. Krishnamoorthy, M. Rao, and S. Mayor. 2004. Nanoscale organization of multiple GPI-anchored proteins in living cell membranes. *Cell.* 116:577–589.

Simons, K., and E. Ikonen. 1997. Functional rafts in cell membranes. *Nature.* 387:569–572.

Sohn, H.W., P. Tolar, T. Jin, and S.K. Pierce. 2006. Fluorescence resonance energy transfer in living cells reveals dynamic membrane changes in the initiation of B cell signaling. *Proc. Natl. Acad. Sci. USA.* 103:8143–8148.

Tolar, P., H.W. Sohn, and S.K. Pierce. 2005. The initiation of antigen-induced BCR signaling viewed in living cells by FRET. *Nat. Immunol.* 6:1168–1176.

van Rheenen, J., M. Langeslag, and K. Jalink. 2004. Correcting confocal acquisition to optimize imaging of fluorescence resonance energy transfer by sensitized emission. *Biophys. J.* 86:2517–2529.

Zal, T., and N.R. Gascoigne. 2004. Photobleaching-corrected FRET efficiency imaging of live cells. *Biophys. J.* 86:3923–3939.